Conclusions

Based on our laboratory measurements and the preceding analysis, it is reasonable to conclude that interactions between operating space vehicles and the space environment can produce surfaces with significantly and even drastically altered SEE characteristics over time scales much less than spacecraft lifetimes. Further, it is important to emphasize that these changes are occurring as a result of the deposition and removal of surface films on the order of only 1 nm, i.e., tens of atoms, thick. Although the ESD and ESA observed in our laboratory are not likely to be the prime mechanisms for the surface modifications that occur on spacecraft surfaces, other mechanisms produce, at comparable rates, surface modifications similar to those observed in this investigation; it is reasonable to assume that the resulting effects on secondary electron yields will be comparable. Of concern to spacecraft designers and controllers should be the fact that these changes in SE yields lead to significant changes in a spacecraft's equilibrium potential in a given charging environment. The results of this investigation have clearly demonstrated the need for a systematic, quantitative study of the dynamic evolution of the SEE characteristics of spacecraft surfaces due to space environment effects. Specifically, such study is necessary if present charging codes are to accurately assess the electric potentials to which spacecraft may be subject over their entire operational lifetimes.

Acknowledgments

This work was supported by fellowships from NASA's Rocky Mountain Space Grant Consortium and by the NASA Graduate Student Researcher's Program. Additionally, we gratefully acknowledge the contributions of John Raitt and Jan Sojka of the Utah State University Physics Department.

References

[1]Katz, I., Mandell, M., Jongeward, G., and Gussenhoven, M. S., "The Importance of Accurate Secondary Electron Yields in Modeling Spacecraft Charging," *Journal of Geophysical Research*, Vol. 91, No. A12, 1986, pp. 13,739–13,744.

[2]Frooninckx, T. B., and Sojka, J. J., "Solar Cycle Dependence of Spacecraft Charging in Low Earth Orbit," *Journal of Geophysical Research*, Vol. 97, No. A3, 1992, pp. 2985–2996.

[3]Garrett, H. B., "The Charging of Spacecraft Surfaces," *Reviews of Geophysics and Space Physics*, Vol. 19, No. 4, 1981, pp. 577–616.

[4]Davies, R. E., "An Instrument for Experimental Secondary Electron Emission Investigations, with Application to the Spacecraft Charging Problem," M.S. Thesis, Dept. of Physics, Utah State Univ., Logan, UT, May 1996.

[5]Dionne, G. F., "Effects of Secondary Electron Scattering on Secondary Emission Yield Curves," *Journal of Applied Physics*, Vol. 44, No. 12, 1973, p. 5361.

[6]Ramsier, R. D., and Yates, J. T., Jr., "Electron-Stimulated Desorption: Principles and Applications," *Surface Science Reports*, Vol. 12, Nos. 6–8, 1991, pp. 247–378.

[7]Smith, T., "Auger Electron Spectroscopy and Ion Sputter Profiles of Oxides on Aluminum," *Surface Science*, Vol. 55, No. 2, 1976, pp. 601–624.

[8]Hillier, J., "On the Investigation of Specimen Contamination in the Electron Microscope," *Journal of Applied Physics*, Vol. 18, March 1948, pp. 226–230.

[9]van Oostrom, A., "Some Aspects of Auger Microanalysis," *Surface Science*, Vol. 89, Nos. 1–3, 1979, pp. 615–634.

[10]Thomas, S., and Pattinson, E. B., "Range of Electrons and Contribution of Backscattered Electrons in Secondary Production in Aluminum," *Journal of Physics D: Applied Physics*, Vol. 3, No. 3, 1970, p. 349.

[11]Weast, R. C. (ed.), *CRC Handbook of Chemistry and Physics*, 65th ed., CRC Press, Boca Raton, FL, 1984, p. E-352.

[12]Titterington, D. M., Smith, A. F. M., and Makov, U. E., *Statistical Analysis of Finite Mixture Distributions*, Wiley, New York, 1985, p. 114.

[13]Hardy, D. A., Gussehnoven, M. S., and Holeman, E., "A Statistical Model of Auroral Electron Precipitation," *Journal of Geophysical Research*, Vol. 90, No. A5, 1985, pp. 4229–4248.

[14]Gussehnoven, M. S., and Mullen, E. G., "Geosynchronous Environment for Severe Spacecraft Charging," *Journal of Spacecraft and Rockets*, Vol. 20, No. 1, 1983, pp. 26–34.

[15]Crutcher, E. R., Nishimura, L. S., Warner, K. J., and Wascher, W. W., "Migration and Generation of Contaminants from Launch Through Recovery: LDEF Case History," *LDEF—69 Months in Space, First Post-Retrieval Symposium*, NASA Conf. Pub. 3134, Pt. 1, 1991, pp. 121–140.

[16]Crutcher, E. R., Nishimura, L. S., Warner, K. J., and Wascher, W. W., "Quantification of Contaminants Associated with LDEF," *LDEF—69 Months in Space, First Post-Retrieval Symposium*, NASA Conf. Pub. 3134, Pt. 1, 1991, pp. 141–177.

A. C. Tribble
Associate Editor

Optimization of a Dual-Mixture-Ratio Hydrogen-Fuel Rocket

Lorenzo Casalino*
Politecnico di Torino, Turin 10129, Italy

Introduction

THE variable mixture ratio is an appealing means of improving rocket performance as it allows the engine to operate with a high mixture ratio, i.e., high thrust-to-weight ratio and propellant bulk density, at low altitude and with a low mixture ratio, i.e., high specific impulse, at high altitude,[1] thus reducing the rocket dry mass. In a previous paper,[2] the rocket performance, in the absence of gravitational and aerodynamic forces, was optimized by considering a continuously varying mixture ratio. The significant benefit, in terms of payload increase or dry-mass reduction, suggests that the control of the mixture ratio could be a means of making a single-stage-to-orbit (SSTO) vehicle feasible. In the present Note, dual mixture ratio is considered, as it presents a lower operational complexity and can permit a comparable benefit.

Statement of the Problem

The rocket operation is considered as being divided into two (or more) phases with a different mixture ratio, which is, however, constant during each phase. In a vacuum, if a rocket with mass m is only subject to its thrust T, the relevant equations, in the jth phase, are

$$\frac{\mathrm{d}m}{\mathrm{d}t} = -\frac{p_c A_t}{c_j^*} \tag{1}$$

$$\frac{\mathrm{d}m_h}{\mathrm{d}t} = \frac{p_c A_t}{c_j^*}\frac{1}{1+\alpha_j} \tag{2}$$

$$\frac{\mathrm{d}V}{\mathrm{d}t} = \frac{T_j}{m} = \frac{p_c A_t}{c_j^*}\frac{c_j}{m} \tag{3}$$

The engine characteristics, i.e., the combustion chamber pressure p_c, and the nozzle geometry, in terms of throat area A_t and expansion area ratio, are considered as being assigned. Equation (1) relates the rocket mass reduction to the propellant flow rate, which is expressed as a function of the mixture ratio α_j (oxidizer/fuel mass ratio) via the characteristic exhaust velocity c_j^*. Equation (2) relates the hydrogen (subscript h) flow rate to the propellant flow rate by means of the mixture ratio, whereas Eq. (3) relates the velocity V increment to the effective exhaust velocity c_j, which is only a function of α_j. The mixture ratio is constant in each phase, and Eqs. (1–3) can be analytically integrated to obtain the values of m, m_h, and V as a function of t once α_j is given.

The optimization consists in the determination of the time length and mixture ratio for each phase to maximize a given performance index φ while obtaining an assigned value for the final velocity V_f; by assuming the rocket initial mass is unitary, the minimization of

Received March 24, 1997; accepted for publication April 8, 1997.

*Researcher, Dipartimento di Energetica.

the gross mass per unit payload (which is related to the mission feasibility) is equivalent to maximizing the payload itself:

$$\varphi = m_u = m_f - m_e - m_t$$
$$= (1 + k_o)\, m_{pf} - (k_h - k_o)\, m_{hf} - k_o - m_e \tag{4}$$

where m_t is the tank mass (proportional to the propellant volumes and, therefore, to the propellant masses via the constants k_h for the fuel and k_o for the oxidizer) and m_e is the engine mass, which also includes all other masses that are independent of the propulsion requirements. Subscript f indicates the final value. On the other hand, if the dry mass m_f (related to the system costs) per unit payload is minimized, the performance index that must be maximized is the payload/dry-mass ratio,

$$\varphi = \frac{m_u}{m_f} = 1 + k_o - \frac{(k_h - k_o)\, m_{hf} + k_o + m_e}{m_f} \tag{5}$$

The parameters of the optimization are the mixture ratio and the time length of each phase, and the performance index depends on the parameters via the final values m_{hf} and m_f. The optimal values can be obtained by nullifying the performance index derivatives with respect to the parameters and by numerically solving the nonlinear algebraic system that arises.

In the present approach, to exploit the theory of optimal control, the Hamiltonian is defined as

$$H = \frac{p_c A_t}{c_j^*}\left(\frac{\lambda_h}{1+\alpha_j} + \frac{\lambda_V c_j}{m} - \lambda_m\right) \tag{6}$$

On the basis of the Euler–Lagrange equations,[3] the adjoint variables λ_h and λ_V result to be constant, whereas in the jth phase,

$$\frac{\mathrm{d}\lambda_m}{\mathrm{d}t} = -\frac{\partial H}{\partial m} = -\frac{p_c A_t}{c_j^*}\frac{\lambda_V c_j}{m^2} \tag{7}$$

The problem is completed by the boundary conditions: if the integration interval is split into phases that experience homogeneous control law, a general expression for the optimal conditions at the junctions can be obtained.[3,4] The initial values ($t = 0$) for Eqs. (1–3) are $m_0 = 1$ and $m_{h0} = V_0 = 0$. Moreover, the final velocity $V_f = \Delta V$ is prescribed.

The rocket and hydrogen final masses are not specified, and the necessary conditions for optimality are[3]

$$\lambda_{mf} = \frac{\partial\varphi}{\partial m_f} \tag{8}$$

$$\lambda_{hf} = \frac{\partial\varphi}{\partial m_{hf}} \tag{9}$$

Because neither the performance index nor any constraint involves the independent variable, the Hamiltonian is zero at the final time and continuous at each jump in the mixture ratio. Moreover, the process is autonomous, i.e., not explicitly dependent on time, and the Hamiltonian is constant and, therefore, null during each phase.

To determine the optimal value for the mixture ratio in each phase, the trivial equation $\mathrm{d}\alpha/\mathrm{d}t = 0$ is added and a further adjoint variable λ_α is introduced. The Euler–Lagrange equation, which rules λ_α in each jth phase, is

$$\frac{\mathrm{d}\lambda_\alpha}{\mathrm{d}t} = \frac{p_c A_t}{c_j^*}\left(\frac{\lambda_h}{(1+\alpha_j)^2} - \frac{\lambda_V}{m}\frac{\mathrm{d}c_j}{\mathrm{d}\alpha}\right) \tag{10}$$

as the Hamiltonian is identically null.

The mixture ratio does not appear in the performance index and is not involved in any constraint; therefore, $\lambda_\alpha = 0$ at the initial and final time and at every switch from a constant-α phase to the next one.

The expressions that Eqs. (8) and (9) assume, depending on the performance index, can be found elsewhere.[2] The boundary value problem outlined in this section is solved by means of a procedure[4] based on Newton's method and developed to deal with trajectory optimization. Note that Eq. (10) can be analytically integrated; this analytical solution obviously leads to the same nonlinear algebraic system as the classical approach.

The propellant flow rate $p_c A_t/c_j^*$ is not involved in the optimization procedure and simply appears as a multiplier in each differential equation. Therefore, time could be eliminated by assuming the ejected propellant mass as the new independent variable[2]; the present formulation is, however, preferred as it can easily be extended to the optimization of actual ascent trajectories also to take gravitational and aerodynamic forces into account. The effective exhaust velocity and the propellant flow rate itself are, however, strictly related to the pressure in the combustion chamber.

Numerical Results

Numerical computations have been carried out by assuming $k_h = 16/70$, $k_o = 16/1141$ (ratios between the tank mass per unit volume and propellant bulk density), and $m_e = 0.05$ according to Martin's[5] suggestions (m_e is not identically defined). The effective exhaust velocity in a vacuum has been computed for a 200-bar combustion chamber pressure and an 80 nozzle expansion area ratio, by considering a one-dimensional frozen equilibrium flow, but for the sake of simplicity, it has been approximated by using the parabolic relation $c = c_0 - c_1(\alpha - \alpha^*)^2$, where $\alpha^* = 3.8$, $c_0 = 0.585$, and $c_1 = 3.532 \times 10^{-3}$ (throughout velocities are normalized by using the circular velocity at the Earth surface as the reference value). A numerical solution, however, can be obtained for any different function $c(\alpha)$.

Figure 1 refers to the maximization of the payload/dry-mass ratio for $\Delta V = 1.25$ and shows a parametric study for the two-phase operation. By fixing α_1 and α_2, the optimal switching time is found by means of an ordinary differentiation of the performance index. The higher mixture ratio, i.e., higher consumption of the oxidizer, which presents higher bulk density and, therefore, a lighter tank per

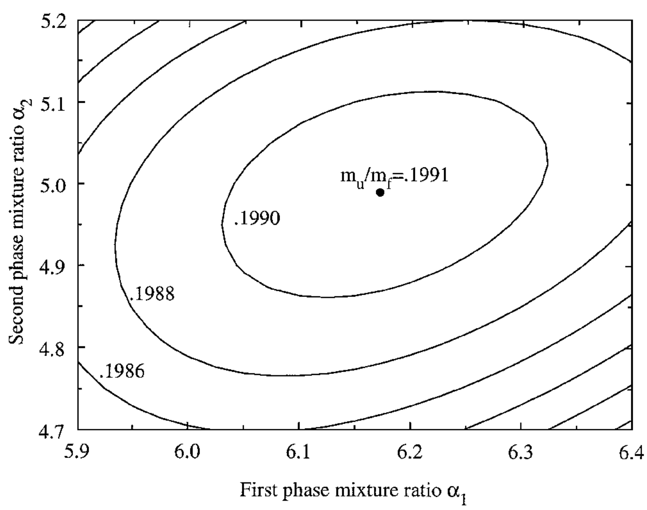

Fig. 1 Payload/dry-mass ratio for two-phase operation.

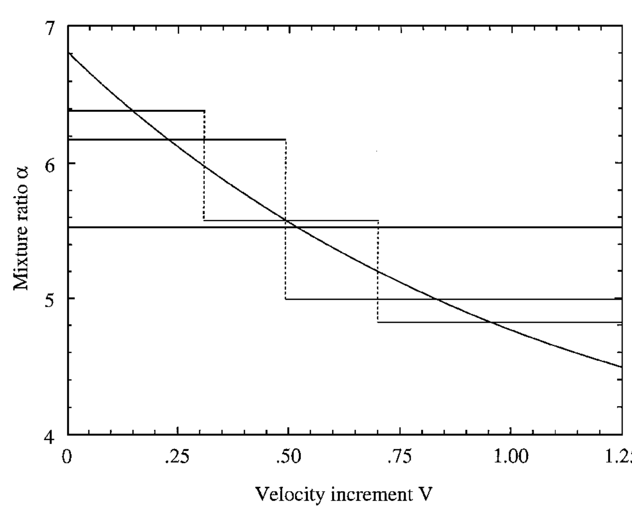

Fig. 2 Control histories for maximum payload/dry-mass ratio.

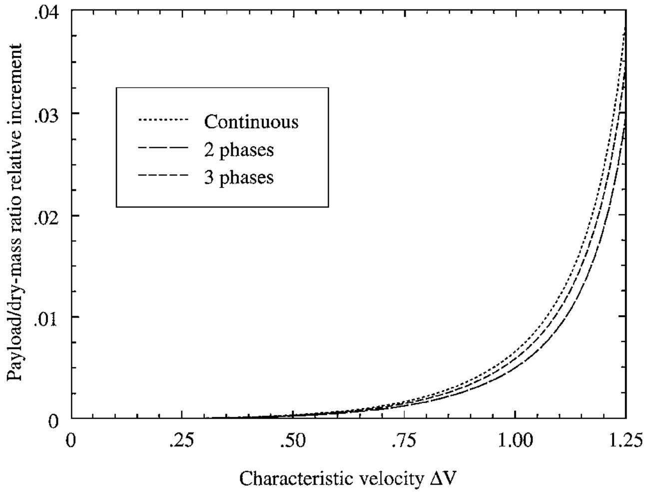

Fig. 3 Payload/dry-mass ratio increment.

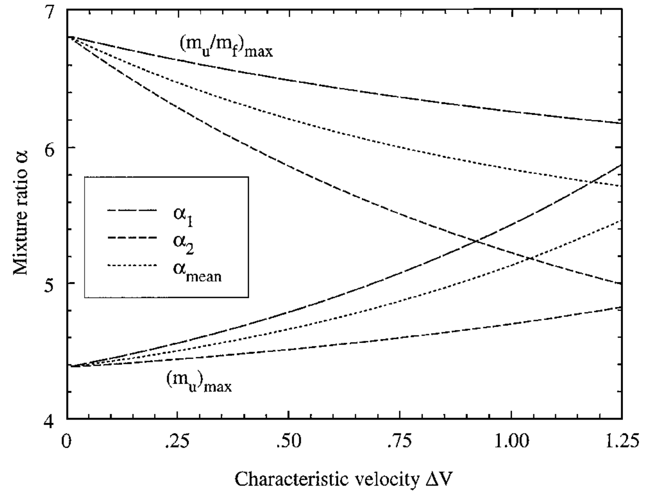

Fig. 4 Maximum payload and payload/dry-mass ratio comparison.

unit mass, is always used in the initial phase to reduce the tank mass, whereas the lower mixture ratio, i.e., higher specific impulse, is used in the final phase where, due to the rocket mass reduction, most of the acceleration is obtained.

Figure 2 shows the mixture ratio as a function of the velocity increment when the same final velocity ($\Delta V = 1.25$) is achieved using an increasing number of constant-α phases and, eventually, a continuously variable mixture ratio. The mean mixture ratio increases with the number of phases from 5.52 to 5.77 and moves far from the value $\alpha^* = 3.8$, which corresponds to the highest specific impulse; the increasing number of phases allows one to exploit a larger range of mixture ratios, thus increasing the effects of the tank mass reduction (first phase) and the exploitation of the higher specific impulse (final phase). The performance index, therefore, increases with the number of phases, as can be seen in Fig. 3, which presents the relative increment of the payload/dry-mass ratio with respect to the constant-α operation as a function of the characteristic velocity ΔV. Most of the benefit, however, is obtained by passing from a one-phase to a two-phase operation (whose mean mixture ratio is 5.72). The dual mixture ratio presents a further advantage in that the range of the exploited mixture ratio is smaller, with lower operational complexity. It is evident that the variable mixture ratio operation is appealing for the most demanding missions.

Figure 4 compares the mixture ratio for the maximum payload and maximum payload/dry-mass ratio: for a low-ΔV operation the control strategies are very different, whereas they become similar for marginal missions. The maximization of the payload/dry-mass ratio always implies a higher mean mixture ratio, i.e., lower tank masses.

A comparison of the results suggests that the use of either performance index is the same for high-ΔV missions, where the greatest benefit of the mixture ratio control can be obtained. In contrast, the control law is quite different if the velocity increment is moderate.

Conclusions

Rocket performance in the absence of gravitational and aerodynamic forces has been optimized by means of an indirect method by considering the engine operation divided into phases with different constant mixture ratios. The benefit, in terms of payload and payload/dry-mass ratio, is significant for the most demanding missions, when the optimal strategy is almost independent of the performance index, which is maximized. In contrast, if the characteristic velocity is low, the performance improvement is moderate and the control strategies are quite different.

The results suggest that, by operating the engine with two different values of the mixture ratio (the higher in the initial phase, the lower in the final phase), a significant benefit is obtained. This control strategy is simple and seems to be a promising means of improving launch system performance and, in the near future, of making an SSTO vehicle feasible.

References

[1] Martin, J. A., and Manski, D., "Variable-Mixture-Ratio and Other Rocket Engines for Advanced Shuttles," *Journal of Propulsion and Power*, Vol. 7, No. 4, 1991, pp. 549–555.

[2] Colasurdo, G., Pastrone, D., and Casalino, L., "Mixture-Ratio Control to Improve Hydrogen-Fuel Rocket Performance," *Journal of Spacecraft and Rockets*, Vol. 34, No. 2, 1997, pp. 214–217.

[3] Bryson, A. E., and Ho, Y.-C., *Applied Optimal Control*, revised, Hemisphere, Washington, DC, 1975, pp. 47–55, 101–108.

[4] Colasurdo, G., and Pastrone, D., "Indirect Optimization Method for Impulsive Transfers," *Proceedings of the AIAA/AAS Astrodynamics Conference*, AIAA, Washington, DC, 1994, pp. 441–448.

[5] Martin, J. A., "Comparing Hydrogen and Hydrocarbon Booster Fuels," *Journal of Spacecraft and Rockets*, Vol. 25, No. 1, 1988, pp. 92–94.

J. A. Martin
Associate Editor